

Electronic Supplementary Information (ESI)

New strategy of achieving single-molecular white-light emission: using vibration-induced emission (VIE) plus aggregation-induced emission (AIE) mechanism as a two-pronged approach

Huan Wang,^a Yiru Li,^a Yiyao Zhang,^a Ju Mei,^{*a} and Jianhua Su^{*a}

a Key Laboratory for Advanced Materials and Institute of Fine Chemicals, School of Chemistry & Molecular Engineering, East China University of Science & Technology, Shanghai 200237, P.R. China. Fax: (86)21-64252288; Tel: (86)21-64252288; E-mail: bbsjh@ecust.edu.cn, daisymeiju@ecust.edu.cn

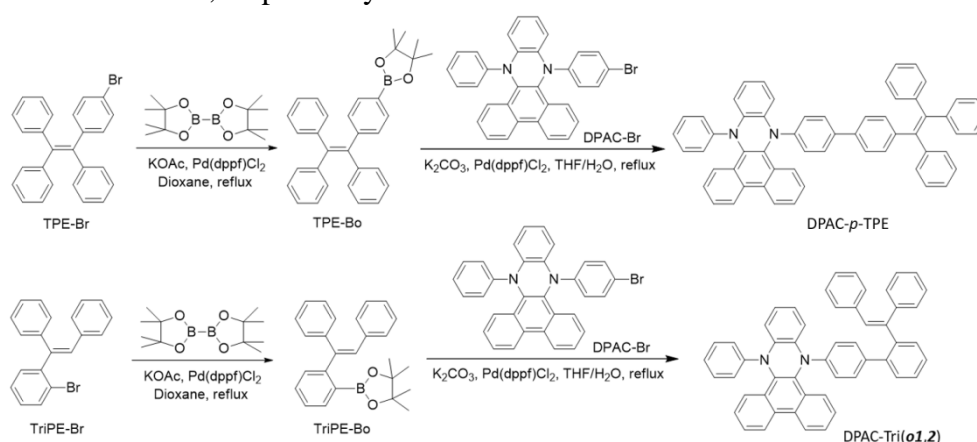
Contents

1. Materials and Methods. (Pages 3 and 4)
2. **Fig. S1** ^1H NMR spectrum of DPAC-*p*-TPE in CDCl_3 . (Page 5)
3. **Fig. S2** ^{13}C NMR spectrum of DPAC-*p*-TPE in CDCl_3 . (Page 5)
4. **Fig. S3** The HRMS of DPAC-*p*-TPE. (Page 6)
5. **Fig. S4** ^1H NMR spectrum of DPAC-Tri(*oI,2*) in CDCl_3 . (Page 6)
6. **Fig. S5** ^{13}C NMR spectrum of DPAC-Tri(*oI,2*) in CDCl_3 . (Page 7)
7. **Fig. S6** The HRMS of DPAC-Tri(*oI,2*). (Page 7)
8. **Fig. S7** The single-crystal structure of DPAC-Tri(*oI,2*). (Page 8)
9. **Table S1**. Crystal data and structure refinement for DPAC-Tri(*oI,2*). (Pages 8 and 9)
10. **Fig. S8** Photoluminescence spectra of solid powders of DPAC-*p*-TPE and DPAC-Tri(*oI,2*), $\lambda_{\text{ex}} = 365$ nm. (Page 9)
11. **Fig. S9** Photoluminescence spectra of DPAC-*p*-TPE (a) and DPAC-Tri(*oI,2*) (b) in different solvents (10^{-5} M), $\lambda_{\text{ex}} = 365$ nm. (Page 9)
12. **Table S2** Quantum yields of DPAC-*p*-TPE and DPAC-Tri(*oI,2*) in different solvents. (Page 9)
13. **Fig. S10** Photoluminescence spectra of TPE-Ph (a), DPAC (b), mixture of TPE-Ph and DPAC (1:1) (c) in toluene with different volume fractions of polyTHF, concentration: 10^{-5} M, $\lambda_{\text{ex}} = 365$ nm. (Page 10)
14. **Fig. S11** The corresponding CIE coordinates of DPAC-*p*-TPE in polyTHF-toluene solutions with different polyTHF fractions. (Page 10)
15. **Fig. S12** Photoluminescence spectra of DPAC-Tri(*oI,2*) (10^{-5} M) in toluene with different volume fractions of polyTHF, $\lambda_{\text{ex}} = 365$ nm. (Page 11)
16. **Table S3** Quantum yields of DPAC-*p*-TPE and DPAC-Tri(*oI,2*) in toluene solutions with different volume fractions of polyTHF and solidified polyTHF. (Page 11)
17. **Fig. S13** Photoluminescence spectra of DPAC-*p*-TPE (10^{-5} M) in THF with different volume fractions of water, $\lambda_{\text{ex}} = 365$ nm. (Page 11)
18. **Fig. S14** Photoluminescence spectra of DPAC-Tri(*oI,2*) (10^{-5} M) in THF with the water fraction of 0–60 vol% (left) and 70–90 vol% (right), $\lambda_{\text{ex}} = 365$ nm. (Page 12)
19. **Table S4** Quantum yields of DPAC-*p*-TPE and DPAC-Tri(*oI,2*) in water-THF solutions with different water fractions. (Page 12)
20. **Fig. S15** The corresponding CIE coordinates of DPAC-Tri(*oI,2*) (10^{-5} M) in THF with different water fractions. (Page 12)
21. **Fig. S16** Schematic illustration of the photophysical behaviors and molecular conformations of DPAC-Tri(*oI,2*) in solution state (upper panel) and the aggregated state (lower panel); IR: intramolecular rotations; RIR: restricted intramolecular rotations. (Page 13)
22. **Fig. S17** DLS results of DPAC-Tri(*oI,2*) (10^{-5} M) in 70 vol% water-THF solution (left) and 90 vol% water-THF solution (right). (Page 13)

General information

DPAC and DPAC-Br were synthesized according to our previous work.[36] Other reagents used for the synthesis or measurements were commercially available without further purification. Water used in tests was ultrapure. THF and toluene were dried with 4 Å molecular sieves and further distilled for the related experiments. PolyTHF (average $M_n \sim 850$) was used as the viscous solvent. PolyTHF (average $M_n \sim 1000$ and $M_n \sim 2000$) were used to make solid mold at 20 °C.

The ^1H NMR and ^{13}C NMR spectra were recorded on a Bruker AM 400 spectrometer with tetramethylsilane as an internal reference. Molecular masses were determined by a Waters LCT premier XE spectrometer. The UV-Vis absorption spectra and PL spectra were performed on a Varian Cray 500 spectrophotometer and a Horiba Fluoromax 4, respectively.



Material synthesis

4,4,5,5-Tetramethyl-2-(4-(1,2,2-triphenylvinyl)phenyl)-1,3,2-dioxaborolane (TPE-Bo). A mixture of TPE-Br (2000.0 mg, 4.0 mmol), bisdiboron (2000.0 mg, 8.0 mmol), KOAc (980.0 mg, 10.0 mmol) and Pd(dppf)Cl₂ (292.7 mg, 0.4 mmol) in 50 mL dried dioxane was refluxed under nitrogen atmosphere for 16h. After cooling to room temperature, the mixture was evaporated and then washed with brine and extracted with ethyl acetate twice. The organic layers were combined and dried over anhydrous Na₂SO₄, filtered and evaporated. The residue was subjected to column chromatography with ethyl acetate/petroleum ether (1/20~1/2, v/v) as eluent. TPE-Bo was obtained as a white solid. Yield: 75%. ^1H NMR (400 MHz, CDCl₃) δ : 7.54 (d, $J = 8.2$ Hz, 2H), 7.11–7.06 (m, 9H), 7.05 – 6.98 (m, 8H), 1.31 (s, 12H).

(*E*)-2-(2-(1,2-Diphenylvinyl)phenyl)-4,4,5,5-tetramethyl-1,3,2-dioxaborolane (TriPE-Bo). The synthetic procedure of TriPE-Bo was totally the same as that of TPE-Bo. TriPE-Bo was obtained as a white solid. Yield: 60%. ^1H NMR (400 MHz, CDCl₃) δ : 7.74–7.64 (m, 1H), 7.32–7.26 (m, 2H), 7.26–7.20 (m, 5H), 7.17–7.06 (m, 6H), 6.54 (s, 1H), 1.15 (s, 12H).

9-Phenyl-14-(4'-(1,2,2-triphenylvinyl)-[1,1'-biphenyl]-4-yl)-9,14-dihydrodibenzo[*a,c*]phenazine (DPAC-*p*-TPE). A mixture of TPE-Bo (458.0 mg, 1.0 mmol),

DPAC-Br (513.0 mg, 1.0 mmol), Pd(dppf)Cl₂ (73.0 mg, 0.1 mmol) and potassium carbonate aqueous solution (2 M, 2 mL) in 30 mL THF was refluxed under nitrogen atmosphere for 8 h. After cooling to room temperature, the mixture was evaporated and then washed with brine and extracted with ethyl acetate twice. The organic layers were combined and dried over anhydrous Na₂SO₄, filtered and evaporated. The residue was subjected to column chromatography with ethyl acetate/petroleum ether (1/20~1/10, v/v) as eluent. DPAC-*p*-TPE was obtained as a pale-yellow solid. Yield: 51%. ¹H NMR (400 MHz, CDCl₃) δ: 8.74 (d, *J* = 8.4 Hz, 2H), 8.10 (dd, *J* = 12.0, 4.4 Hz, 2H), 7.74 (ddd, *J* = 12.0, 7.6, 3.2 Hz, 2H), 7.64 (td, *J* = 8.4, 4.4 Hz, 2H), 7.54 (t, *J* = 7.6 Hz, 2H), 7.38–7.31 (m, 2H), 7.26–7.15 (m, 4H), 7.13–6.90 (m, 23H), 6.82–6.75 (m, 1H); ¹³C NMR (101 MHz, CDCl₃) δ: 147.62, 146.80, 144.74, 144.60, 143.85, 143.79, 141.98, 140.82, 140.63, 138.17, 138.12, 137.82, 132.95, 131.69, 131.42, 131.37, 131.33, 129.92, 129.44, 129.30, 128.84, 127.74, 127.64, 127.62, 127.41, 127.26, 127.05, 127.00, 126.55, 126.41, 126.36, 125.43, 125.39, 124.63, 124.60, 123.06, 123.04, 121.12, 116.84, 116.74; HRMS: [M+H]⁺ calculated for C₅₈H₄₁N₂: 765.3270, found: 765.3262.

(*E*)-9-(2'-(1,2-diphenylvinyl)-[1,1'-biphenyl]-4-yl)-14-phenyl-9,14-dihydrodibenzo[*a,c*]phenazine (DPAC-Tri(*oI,2*)). The synthetic procedure of DPAC-Tri was totally the same as that of DPAC-*p*-TPE. DPAC-Tri was obtained as a white solid. Yield: 47%. ¹H NMR (400 MHz, CDCl₃) δ: 8.70 (dd, *J* = 8.4, 3.2 Hz, 2H), 8.07 (d, *J* = 7.6 Hz, 1H), 7.93 (d, *J* = 7.6 Hz, 1H), 7.71 (ddd, *J* = 9.2, 7.2, 4.4 Hz, 2H), 7.65–7.55 (m, 2H), 7.52 (t, *J* = 7.4 Hz, 1H), 7.41–7.33 (m, 2H), 7.33–7.26 (m, 4H), 7.15–7.06 (m, 4H), 7.00 (d, *J* = 8.0 Hz, 2H), 6.97–6.89 (m, 4H), 6.85–6.77 (m, 5H), 6.71–6.61 (m, 3H), 6.57 (s, 1H), 6.52 (d, *J* = 7.2 Hz, 2H); ¹³C NMR (101 MHz, CDCl₃) δ: 147.63, 145.65, 144.77, 144.31, 143.80, 143.34, 141.19, 140.10, 137.72, 137.55, 137.48, 134.91, 130.48, 130.28, 130.18, 129.91, 129.83, 129.69, 129.51, 129.36, 129.18, 129.12, 128.80, 127.87, 127.40, 127.31, 126.95, 126.91, 126.76, 126.64, 126.55, 126.39, 126.27, 125.28, 125.08, 124.66, 124.56, 122.97, 122.93, 121.00, 116.49, 116.40; HRMS: [M+H]⁺ calculated for C₅₂H₃₇N₂: 689.2957, found: 689.2963.

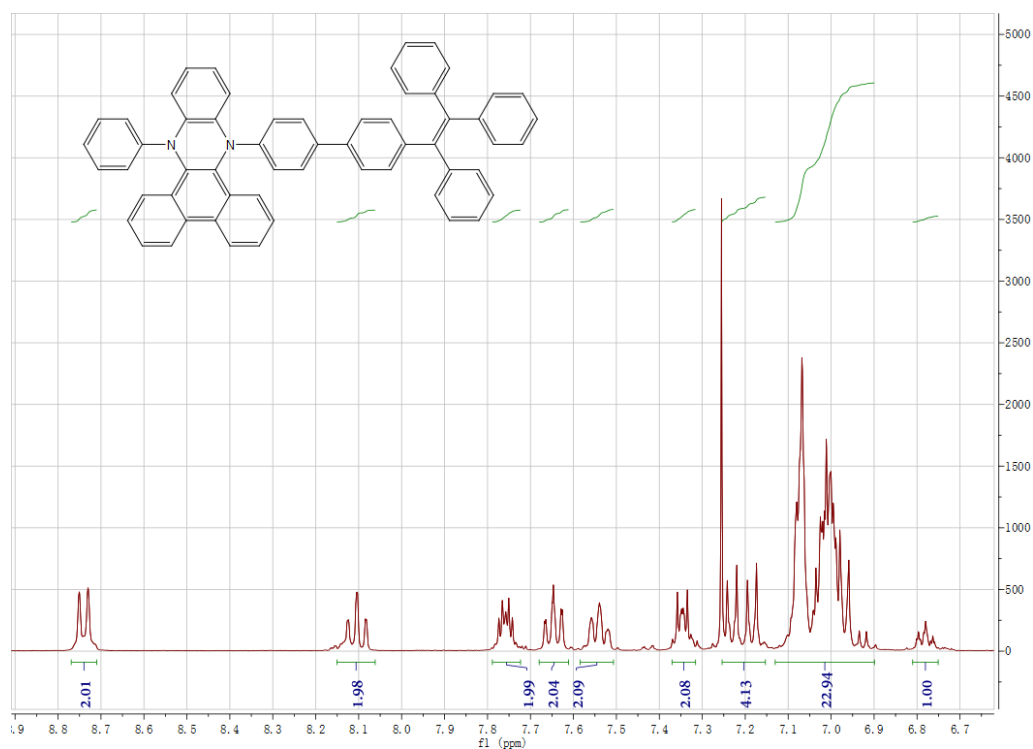


Fig. S1 ^1H NMR spectrum of DPAC-*p*-TPE in CDCl_3 .

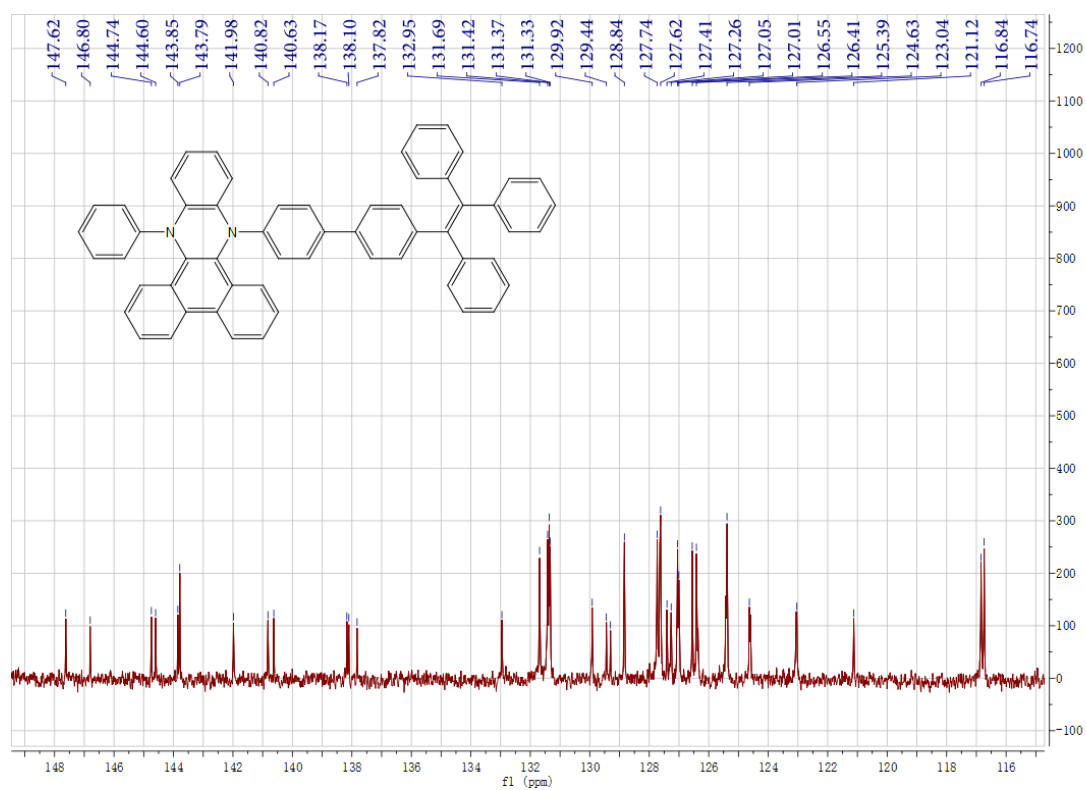


Fig. S2 ^{13}C NMR spectrum of DPAC-*p*-TPE in CDCl_3 .

Single Mass Analysis

Tolerance = 5.0 PPM / DBE: min = -1.5, max = 50.0

Element prediction: Off

Number of isotope peaks used for i-FIT = 2

Monoisotopic Mass, Even Electron Ions

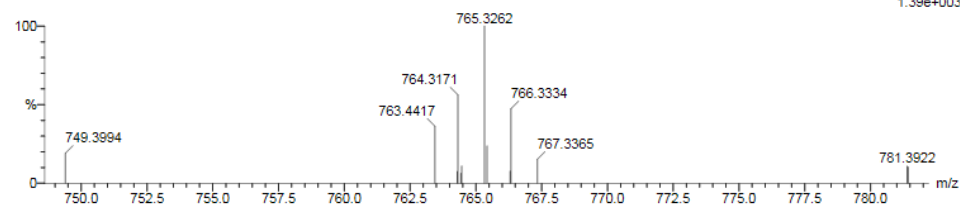
4 formula(e) evaluated with 1 results within limits (up to 50 closest results for each mass)

Elements Used:

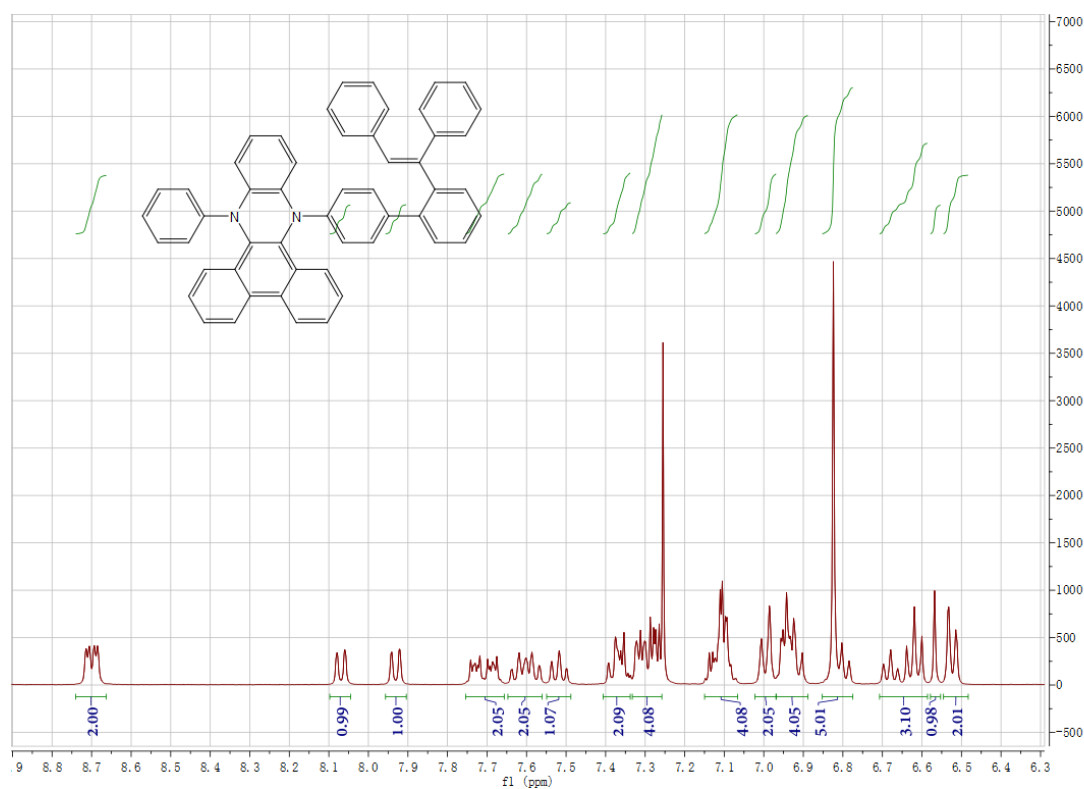
C: 0-58 H: 0-41 N: 0-2 Na: 0-1

JH-SU

TH-WH-01 15 (0.158) Cm (14.21)

1: TOF MS ES+
1.39e+003

Mass	Calc. Mass	mDa	PPM	DBE	i-FIT	i-FIT (Norm)	Formula
765.3262	765.3270	-0.8	-1.0	39.5	35.1	0.0	C58 H41 N2

Fig. S3 The HRMS of DPAC-*p*-TPE.Fig. S4 ¹H NMR spectrum of DPAC-Tri(*o*1,2) in CDCl₃.

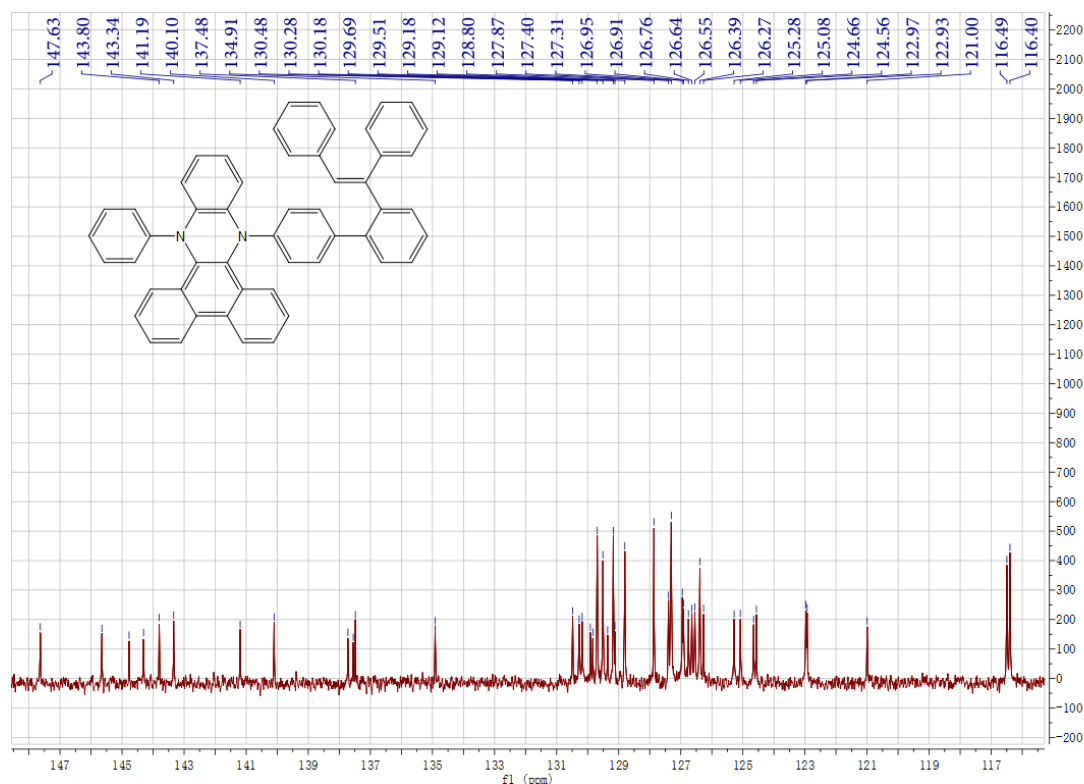


Fig. S5 The ^{13}C NMR spectrum of DPAC-Tri(*o1,2*) in CDCl_3 .

Elemental Composition Report

Page 1

Single Mass Analysis

Tolerance = 5.0 PPM / DBE: min = -1.5, max = 50.0

Element prediction: Off

Number of isotope peaks used for i-FIT = 2

Monoisotopic Mass, Even Electron Ions

4 formula(e) evaluated with 1 results within limits (up to 50 closest results for each mass)

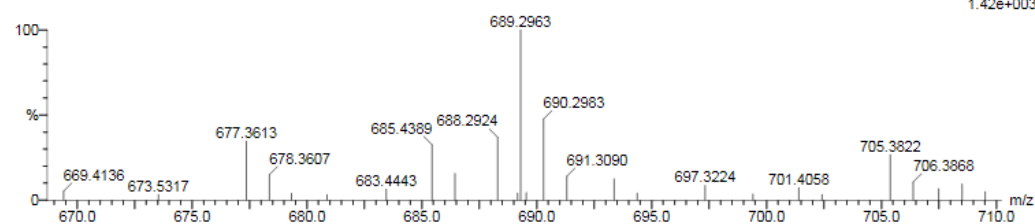
Elements Used:

C: 0-52 H: 0-37 N: 0-2 Na: 0-1

JH-SU

TH-WH-02 33 (0.359) Cm (28:35)

1: TOF MS ES+
1.42e+003



Minimum:

Maximum: 5.0 5.0 -1.5 50.0

Mass	Calc. Mass	mDa	PPM	DBE	i-FIT	i-FIT (Norm)	Formula
689.2963	689.2957	0.6	0.9	35.5	19.8	0.0	C52 H37 N2

Fig. S6 The HRMS of DPAC-Tri(*o1,2*).

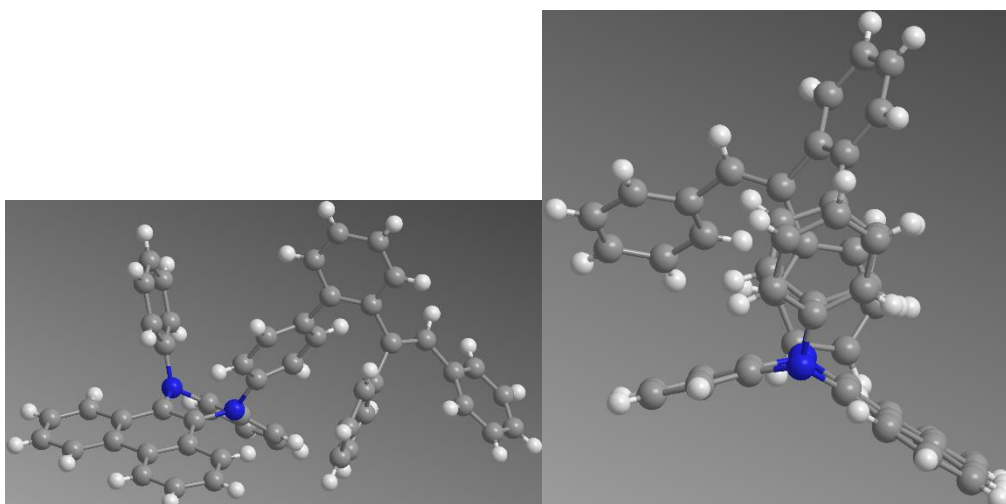


Fig. S7 The single-crystal structure of DPAC-Tri(*o1,2*).

Table S1. Crystal data and structure refinement for DPAC-Tri(*o1,2*).

Empirical formula	C ₅₃ H ₃₈ Cl ₂ N ₂	
Formula weight	773.75	
Temperature	296(2) K	
Wavelength	0.71073 Å	
Crystal system	Triclinic	
Space group	P -1	
Unit cell dimensions	a = 9.4773(9) Å	α = 69.381(3)°
	b = 13.6425(13) Å	β = 75.821(3)°
	c = 17.4442(17) Å	γ = 87.618(3)°
Volume	2044.2(3) Å ³	
Z	2	
Density (calculated)	1.257 Mg/m ³	
Absorption coefficient	0.198 mm ⁻¹	
F(000)	808	
Crystal size	0.200 x 0.170 x 0.130 mm ³	
Theta range for data collection	2.574 to 25.998°	
Index ranges	-11 ≤ h ≤ 11, -16 ≤ k ≤ 16, -21 ≤ l ≤ 21	
Reflections collected	36399	
Independent reflections	7992 [R(int) = 0.0424]	
Completeness to theta = 25.242°	99.3 %	
Absorption correction	Semi-empirical from equivalents	
Max. and min. transmission	0.7456 and 0.6721	
Refinement method	Full-matrix least-squares on F ²	
Data / restraints / parameters	7992 / 0 / 515	

Goodness-of-fit on F ²	1.017
Final R indices [I>2sigma(I)]	R1 = 0.0540, wR2 = 0.1313
R indices (all data)	R1 = 0.0789, wR2 = 0.1505
Extinction coefficient	0.041(5)
Largest diff. peak and hole	0.258 and -0.420 e.Å ⁻³

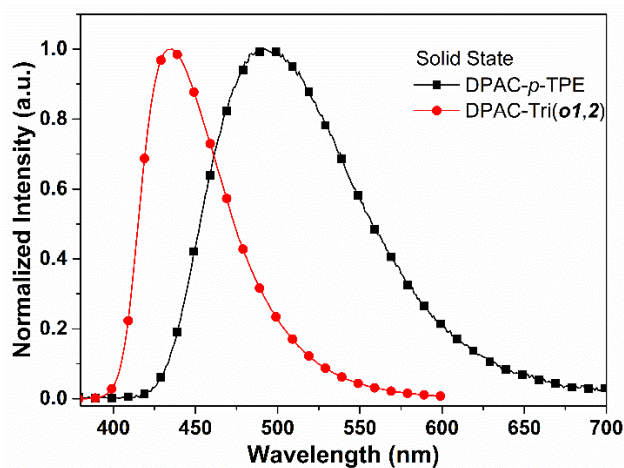


Fig. S8 Photoluminescence spectra of solid powders of DPAC-*p*-TPE and DPAC-Tri(*o*1,2), $\lambda_{\text{ex}} = 365$ nm.

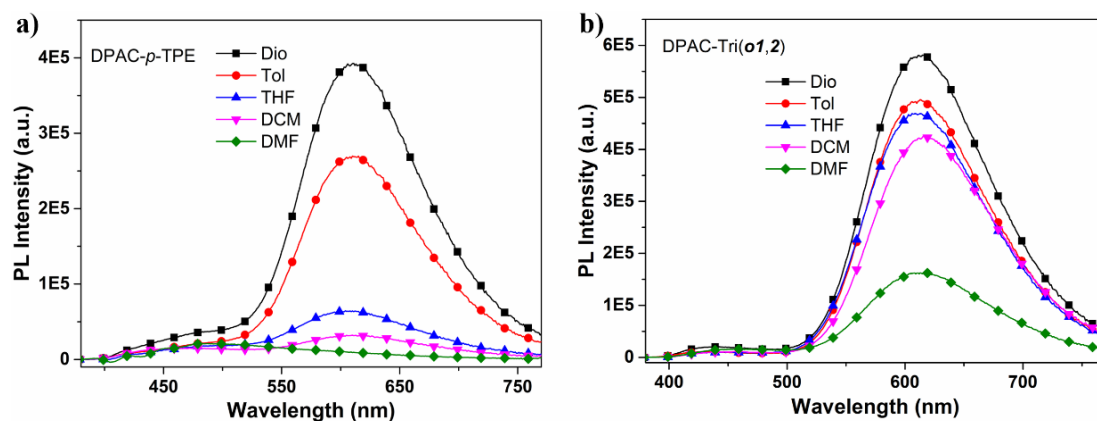


Fig. S9 Photoluminescence spectra of DPAC-*p*-TPE (a) and DPAC-Tri(*o*1,2) (b) in different solvents (10^{-5} M), $\lambda_{\text{ex}} = 365$ nm.

Table S2 Quantum yields of DPAC-*p*-TPE and DPAC-Tri(*o*1,2) in different solvents.

Compound	Q.Y. ^a (Dio, %)	Q.Y. ^a (Tol, %)	Q.Y. ^a (THF, %)	Q.Y. ^a (DCM, %)	Q.Y. ^a (DMF, %)
DPAC- <i>p</i> -TPE	1.0	0.7	0.3	0.1	0.1
DPAC-Tri(<i>o</i> 1,2)	3.8	3.1	3.0	2.8	1.3

^aQ.Y. = quantum yield, tested by the Horiba integrating sphere.

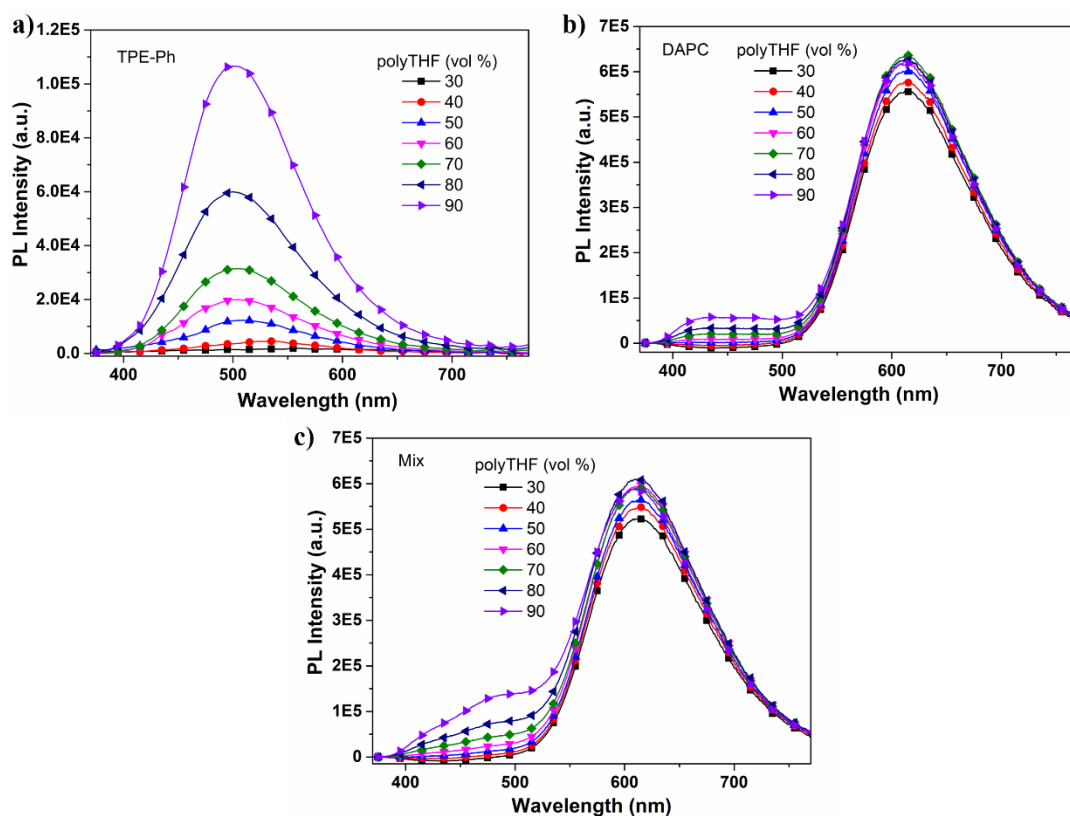


Fig. S10 Photoluminescence spectra of TPE-Ph (a), DPAC (b), mixture of TPE-Ph and DPAC (1:1) (c) in toluene with different volume fractions of polyTHF, concentration: 10^{-5} M, $\lambda_{\text{ex}} = 365$ nm.

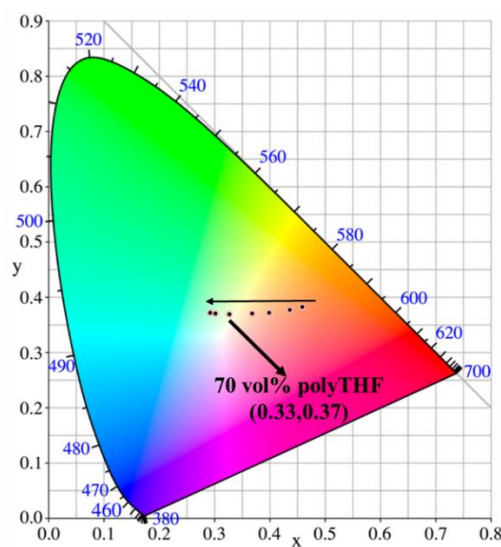


Fig. S11 The corresponding CIE coordinates of DPAC-*p*-TPE in polyTHF-toluene solutions with different polyTHF fractions.

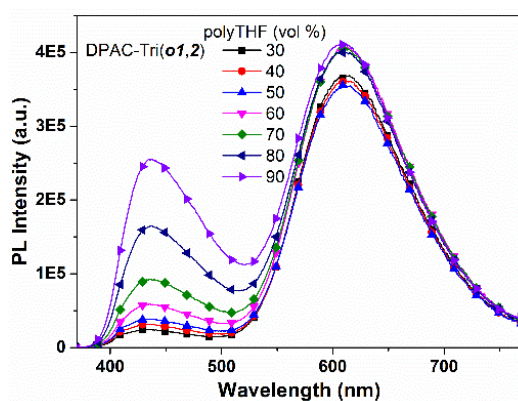


Fig. S12 Photoluminescence spectra of DPAC-Tri(*o1,2*) (10^{-5} M) in toluene with different volume fractions of polyTHF. $\lambda_{\text{ex}} = 365$ nm.

Table S3. Quantum yields of DPAC-*p*-TPE and DPAC-Tri(*o1,2*) in toluene solutions with different volume fraction of polyTHF and solidified polyTHF.

Compound	Q.Y. ^a (%)							Q.Y. ^a (pure polyTHF, $M_n \sim 1$ K, %)	Q.Y. ^a (pure polyTHF, $M_n \sim 2$ K, %)
	30	40	50	60	70	80	90		
	vol %	vol %	vol %	vol %	vol %	vol %	vol %		
DPAC- <i>p</i> -TPE	1.0	1.1	1.3	1.5	2.0	2.6	3.2	/	/
DPAC-Tri(<i>o1,2</i>)	3.2	3.2	3.3	3.8	4.0	4.4	5.1	5.8	7.8

^aQ.Y.= quantum yield, tested by the Horiba integrating sphere.

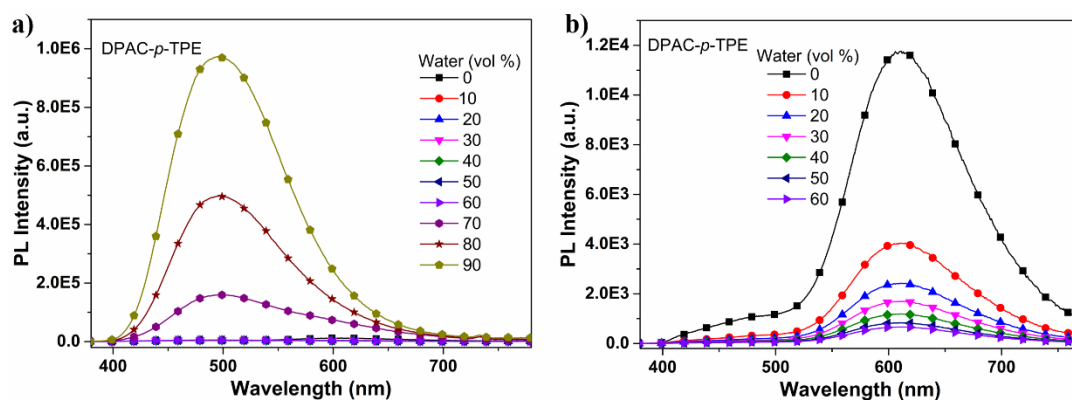


Fig. S13 Photoluminescence spectra of DPAC-*p*-TPE (10^{-5} M) in THF with different volume fractions of water, $\lambda_{\text{ex}} = 365$ nm.

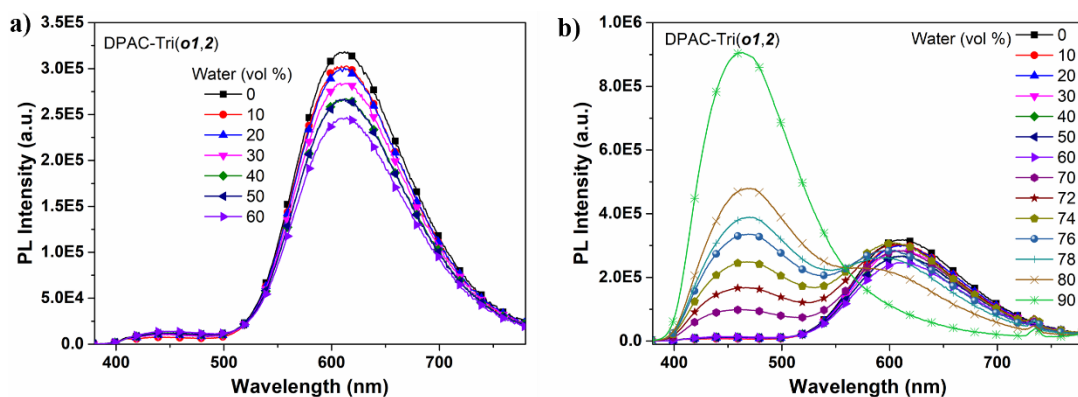


Fig. S14 Photoluminescence spectra of DPAC-Tri(*o1,2*) (10^{-5} M) in THF with the water fraction of 0–60 vol% (a) and 70–90 vol% (b), $\lambda_{\text{ex}} = 365$ nm.

Table S4 Quantum yields of DPAC-*p*-TPE and DPAC-Tri(*o1,2*) in water-THF solutions with different water fractions.

Compound	Q.Y. ^a (% , water fraction/vol %)													
	0	10	20	30	40	50	60	70	72	74	76	78	80	90
DPAC- <i>p</i> -TPE	0.3	0.2	0.2	0.1	0.1	0.1	0.1	3.2	/	/	/	/	8.4	12.3
DPAC-Tri(<i>o1,2</i>)	3.0	2.8	2.8	2.7	2.6	2.5	2.4	3.4	4.1	4.7	5.2	5.3	5.6	8.1

^aQ.Y. = quantum yield, tested by the Horiba integrating sphere.

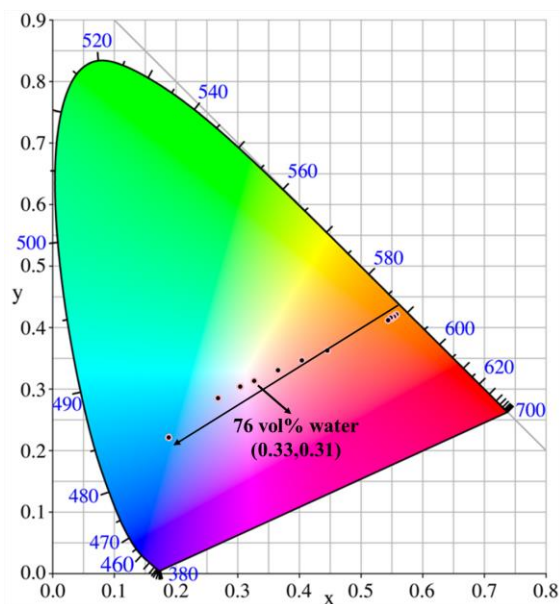


Fig. S15 The corresponding CIE coordinates of DPAC-Tri(*o1,2*) (10^{-5} M) in THF with different water fractions.

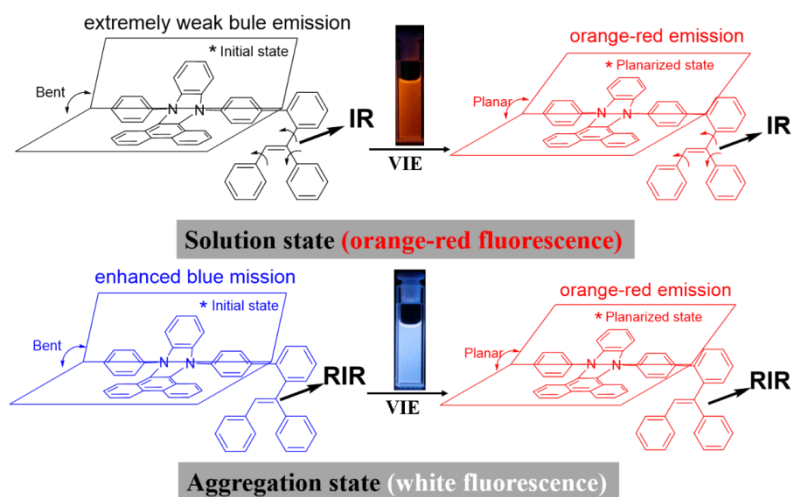


Fig. S16 Schematic illustration of the photophysical behaviors and molecular conformations of DPAC-Tri(o1,2) in solution state (upper panel) and aggregation state (lower panel); IR: intramolecular rotations; RIR: restricted intramolecular rotations.

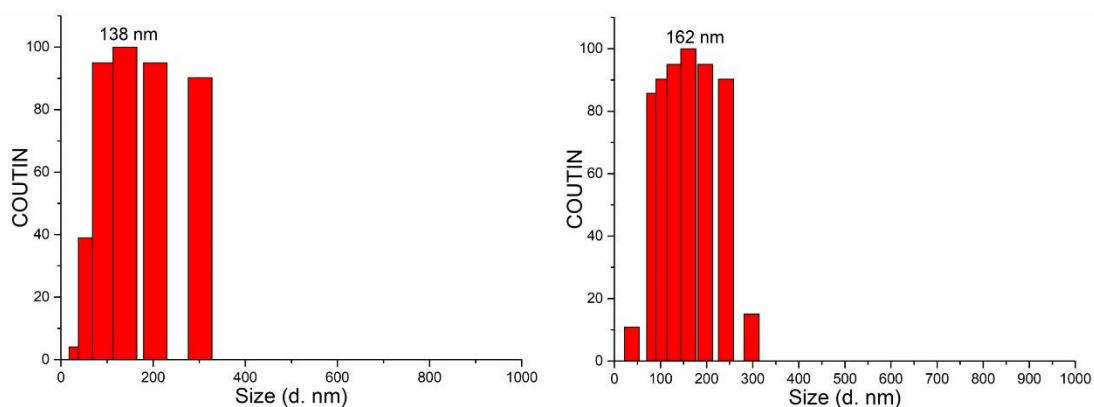


Fig. S17 DLS results of DPAC-Tri(o1,2) (10^{-5} M) in 70 vol% water-THF solution (left) and 90 vol% water-THF solution (right).